Developmental Cell, Vol. 3, 283–289, August, 2002, Copyright ©2002 by Cell Press

Endosome-Associated Complex, ESCRT-II, Recruits Transport Machinery for Protein Sorting at the Multivesicular Body

Markus Babst,[2,4] David J. Katzmann,[4] William B. Snyder,[2] Beverly Wendland,[3] and Scott D. Emr[1]
Department of Cellular and Molecular Medicine and Howard Hughes Medical Institute
School of Medicine
University of California, San Diego
La Jolla, California 92093

Summary

Sorting of ubiquitinated endosomal membrane proteins into the MVB pathway is executed by the class E Vps protein complexes ESCRT-I, -II, and -III, and the AAA-type ATPase Vps4. This study characterizes ESCRT-II, a soluble ~155 kDa protein complex formed by the class E Vps proteins Vps22, Vps25, and Vps36. This protein complex transiently associates with the endosomal membrane and thereby initiates the formation of ESCRT-III, a membrane-associated protein complex that functions immediately downstream of ESCRT-II during sorting of MVB cargo. ESCRT-II in turn functions downstream of ESCRT-I, a protein complex that binds to ubiquitinated endosomal cargo. We propose that the ESCRT complexes perform a coordinated cascade of events to select and sort MVB cargoes for delivery to the lumen of the vacuole/lysosome.

Introduction

The endosomal system of eukaryotic cells receives and sorts cargo proteins from both endocytic and biosynthetic pathways (reviewed in Lemmon and Traub, 2000). In a further level of endosomal sorting, membrane proteins destined for degradation in vacuoles/lysosomes are recognized at the endosome and sorted into multivesicular bodies (MVBs), endosomal structures which form by the invagination and budding of vesicles from the limiting outer membrane into the lumen of the endosome. During this process, a subset of endosomal membrane proteins is sorted into the forming vesicles. After fusion of the MVB with the lysosome/vacuole, the lumenal vesicles, together with their cargo, are exposed to lysosomal hydrolases and degraded (Felder et al., 1990). Proteins that remain in the limiting membrane of the MVB are either recycled to the Golgi complex or the plasma membrane or are delivered to the lysosomal/vacuolar limiting membrane via the fusion of the MVB with this organelle. Therefore, the MVB sorting pathway plays a critical role in the sorting of multiple cargo proteins within the endosomal membrane system.

In a recent study, it has been demonstrated that sorting of the yeast hydrolase carboxypeptidase S (CPS) into the MVB pathway requires monoubiquitination of the short cytoplasmic tail of the protein (Katzmann et al., 2001). Mutations in CPS that block this ubiquitin modification result in mislocalization of the protein to the limiting membrane of the vacuole. Furthermore, a protein complex called ESCRT-I (endosomal sorting complex required for transport) binds to ubiquitinated CPS and thereby directs sorting of the hydrolase into the MVB pathway (Katzmann et al., 2001). ESCRT-I is composed of three different protein subunits (Vps23, Vps28, and Vps37) which belong to the class E vacuolar protein sorting (Vps) proteins, a group of 15 proteins required for proper endosomal function, including the formation of MVBs (Odorizzi et al., 1998). Class E *vps* mutants accumulate large endosomal structures, referred to as "class E compartments," and mislocalize cargoes of the MVB pathway to these structures, as well as the vacuolar membrane.

In addition to ESCRT-I, a set of class E Vps proteins that includes four soluble coiled-coil proteins transiently associates with an endosomal compartment and oligomerize into a protein complex called ESCRT-III (Babst et al., 2002). After ESCRT-III has performed its function in MVB sorting, the AAA-type ATPase Vps4 dissociates the protein complex in an ATP-dependent manner and releases the small coiled-coil proteins from the membrane for further rounds of protein sorting (Babst et al., 1997, 1998).

In this study, we describe the analysis of the class E Vps proteins Vps22, Vps25, and Vps36, which assemble into a soluble protein complex called ESCRT-II. We demonstrate that ESCRT-II transiently associates with endosomes where it is involved in the formation of the protein complex ESCRT-III. Furthermore, we provide evidence that the protein complex ESCRT-I, which binds to ubiquitinated endosomal cargo, acts upstream of ESCRT-II.

Results and Discussion

It has been demonstrated that ubiquitination of membrane proteins in the biosynthetic transport pathway serves as a sorting signal for the MVB-dependent transport of cargo proteins into the lumen of lysosomes/vacuoles (Katzmann et al., 2001; Urbanowski and Piper, 2001). At an endosomal compartment, the ubiquitinated cargo interacts with the protein complex ESCRT-I, which in turn initiates the MVB sorting of the bound cargo by activating the downstream class E Vps protein machinery (Katzmann et al., 2001). A key component of this machinery is ESCRT-III, a protein complex formed on the cytoplasmic face of the endosome which seems to execute the sorting and concentration of the MVB cargo (Babst et al., 2002). The membrane association of ESCRT-III is apparently stabilized by myristoyl groups which are covalently attached to the Vps20 subunits.

[1]Correspondence: semr@ucsd.edu
[2]Present address: MicroGenomics Inc., 5935 Darwin Court, Carlsbad, California 92008.
[3]Present address: Department of Biology, Johns Hopkins University, 3400 North Charles Street, Baltimore, Maryland 21218.
[4]These authors contributed equally to this work.

A

	Molecular Weight [kD]		
	Calculated	SDS-PAGE	Gel filtration
Vps22-HA in WT	31.5 (26.9)*	~30	155
Vps25-HA in WT	28.1 (23.6)*	~30	155
Vps36-HA in WT	68.5 (64.0)*	~70	155
Vps22-HA in *vps36*Δ	31.5	~30	58
Vps36-HA in *vps22*Δ	68.5	~70	53
Vps36-HA in *vps25*Δ	68.5	~70	53
Vps25-HA in *vps36*Δ	28.1	~30	58
ESCRT-II expressed in *E. coli*			155
Vps36 expressed in *E. coli*			55

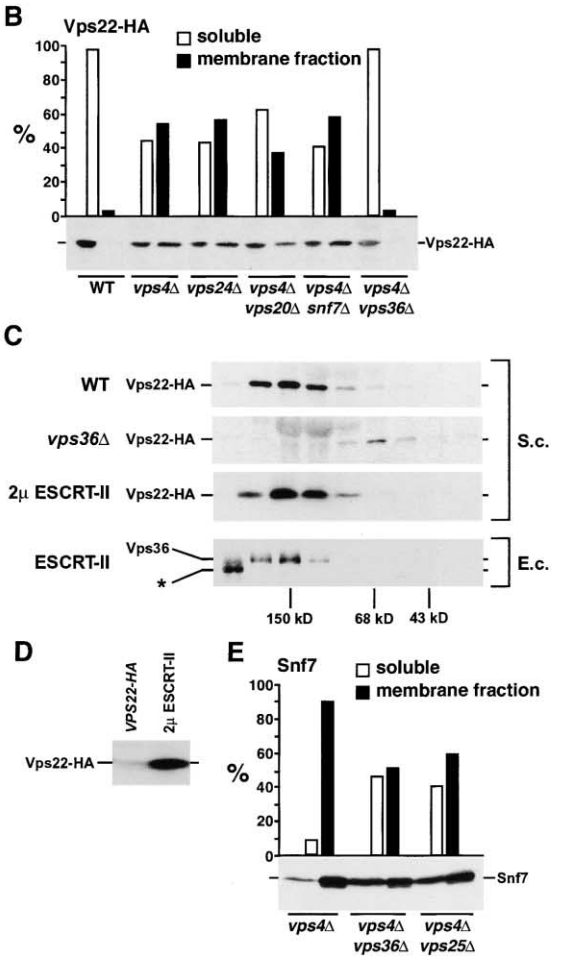

Figure 1. Vps22 Is Part of an ~155 kDa Protein Complex which Transiently Associates with Membranes

(A) Molecular weight of the ESCRT-II subunits determined by SDS-PAGE or gel filtration analysis. Asterisks mark predicted molecular weights of the proteins without an HA tag.

(B) Subcellular fractionation of different yeast strains (see Table 1) expressing Vps22-HA. Cells were spheroplasted and lysed, and the resulting extracts were separated by centrifugation at 13,000 × g into soluble (white bar) and membrane-bound (black bar) pellet fractions. The samples were analyzed for the presence of Vps22-HA by Western blotting using antibodies specific for the HA tag. Quantification of the resulting blot was performed by the Scion Image program (Wayne Rasband, NIH).

(C) Gel filtration analysis of cell extracts from either yeast cells (S.c.) expressing Vps22-HA or *E. coli* (E.c.) expressing ESCRT-II (Xl1-blue pMB202). Yeast strains used for the analysis are: SEY6210 pMB170 (WT), MBY30 pMB170 (*vps36*Δ), and SEY6210 pMB170, pMB175 (2μ ESCRT-II). The yeast samples were analyzed by Western blot for the presence of Vps22-HA using antibodies specific for the HA-tag. The *E. coli* samples were analyzed using anti-Vps36 antibodies. The asterisk indicates a crossreacting protein present in the first lane of the *E. coli* gel filtration analysis.

(D) Western blot analysis of Vps22-HA expressed either from a single copy (*CEN*) plasmid or together with the other ESCRT-II subunits, Vps25 and Vps36, from a high copy (2μ) plasmid. Equivalent OD amounts were loaded in each lane.

(E) Subcellular fractionation of different yeast mutants was performed as described in (B). The fractions were analyzed by Western blot for the presence of Snf7.

After performing its function in MVB sorting, ESCRT-III recruits the AAA-type ATPase Vps4 which catalyzes dissociation of ESCRT-III and recycling of the small coiled-coil proteins for further rounds of sorting (Babst et al., 1998, 2002).

Using immunofluorescence microscopy, we identified among the class E *VPS* gene products three proteins which when altered by mutation dramatically affected the endosomal accumulation of ESCRT-III in *vps4* mutant cells: *VPS36*, a gene that has also been isolated as playing a role in trafficking of the plasma membrane ATPase (Luo and Chang, 2000), *VPS22*, a gene allelic to *SNF8* (hereafter referred to as *VPS22*; Yeghiayan et al., 1995), and a newly identified class E *VPS* gene, *VPS25*. Deletion of each of these genes resulted in mislocalization of vacuolar hydrolases such as CPS and the accumulation of cargo in the class E compartment similar to the trafficking phenotypes of previously characterized class E *vps* mutants (data not shown).

VPS36 encodes an ~65 kDa protein (566 amino acids) with a cysteine-rich motif (four times Cys-X-X-Cys) in the N-terminal region, which may represent a metal binding domain. Vps22 is a small ~30 kDa protein (233 amino acids) containing two predicted coiled-coil domains. Vps25 is ~25 kDa (202 amino acids) in size and has no obvious structural motifs. For immunological detection of these proteins, we fused a hemagglutinin (HA) tag to the 3′ end of each gene. The resulting fusion proteins complemented all vacuolar protein sorting defects of the corresponding deletion mutants, indicating that the fusions were functional at normal expression levels (data not shown). To localize these proteins, cells expressing the HA-tagged fusion proteins were lysed and the resulting cell extracts were separated by centrifugation into soluble and membrane-bound pelletable fractions. Western blot analysis of these fractions indicated that all three proteins were predominantly soluble (Vps22-HA, Figure 1B; Vps25 and Vps36, data not shown). To determine the native molecular weight of the soluble pool of Vps22-HA, Vps25-HA, and Vps36-HA, we performed gel filtration analysis and found that each of these proteins eluted from the column in the size range of approximately 155 kDa, which suggested that these proteins exist in a complex (Figures 1A and 1C). To test this, strains deleted for either *VPS22* or *VPS36* were analyzed by gel filtration. Mutations in *VPS36* resulted in a shift of Vps25 and Vps22 to a smaller molecular weight. Similarly, gel filtration analysis of a *vps22*Δ strain showed a reduced molecular weight of Vps36 (Figure 1A). In addition, deletion of any of the three genes resulted in destabilization of the other gene products, further suggesting that these proteins form a complex (Figure

1C). In the case of Vps25, the protein was dramatically destabilized such that we were not able to detect it in *vps22*Δ cells. To test whether Vps22, Vps25, and Vps36 were sufficient to form the 155 kDa complex, all three genes were cloned into a single 2μ high copy plasmid. Gel filtration analysis of cell lysates from cells transformed with this high copy plasmid contained a >10-fold higher concentration of the 155 kDa complex (Figures 1C and 1D). These data suggested that complex formation is not limited under these conditions, and that these proteins are sufficient to form the 155 kDa complex. This result is further supported by the observation that when expressed in *Escherichia coli*, Vps22, Vps25, and Vps36 were able to form an ~155 kDa protein complex, whereas expression of Vps36 alone in *E. coli* did not result in the formation of the protein complex (Figures 1A and 1C). In addition, mutations in ESCRT-I or ESCRT-III do not affect ESCRT-II formation, indicating that ESCRT-II is formed independently of the other class E Vps protein complexes (data not shown). Together, the data indicated that three class E Vps proteins, Vps22, Vps25, and Vps36, form a soluble ~155 kDa protein complex which we named ESCRT-II (endosomal sorting complex required for transport II). Consistent with this, a recent study described a protein complex isolated from rat liver which consisted of the mammalian homologs of Vps22, Vps25, and Vps36, suggesting that ESCRT-II and its functions are conserved among eukaryotic cells (Kamura et al., 2001).

ESCRT-II Regulates ESCRT-III Formation

Subcellular fractionation of cells deleted for *VPS4* showed that the ESCRT-III subunit Snf7 accumulates in these mutant cells in the pelletable membrane fraction (Babst et al., 1998; Figure 1E). These membranes correspond to aberrant endosomal structures, as shown by colocalization with the endosomal cargo GFP-CPS (Figure 2A). Deletion of ESCRT-II genes such as *VPS25* or *VPS36* in *vps4*Δ cells resulted in redistribution of approximately half of Snf7 to the soluble cytoplasmic fraction (Figure 1E). Furthermore, in these mutant strains, membrane-associated Snf7 was mislocalized to small, non-class E compartments (*vps4*Δ*vps36*Δ, Figure 2A; *vps4*Δ*vps25*Δ, data not shown) and did not colocalize with other ESCRT-III subunits, such as Vps20 (Figure 2B), indicating that proper ESCRT-III formation is impaired.

The ESCRT-III protein complex which accumulates in *vps4*Δ cells can be efficiently purified by native immunoprecipitation (Babst et al., 2002). This is demonstrated in Figure 3A, where Western blot analysis of a sample obtained by immunoprecipitation with antibodies specific for the ESCRT-III subunit Vps20-HA revealed the presence of the subunits Vps24 and Snf7. However, in cells which are deleted for both *VPS4* and an ESCRT-II subunit (e.g., *vps4*Δ*vps36*Δ), the amount of Vps24 and Snf7 which coimmunoprecipitated with Vps20-HA was dramatically reduced (Figure 3A, compare lanes 1 and 2). This result is consistent with the data obtained by immunofluorescence microscopy and suggests that ESCRT-II is required for proper membrane recruitment and assembly of ESCRT-III.

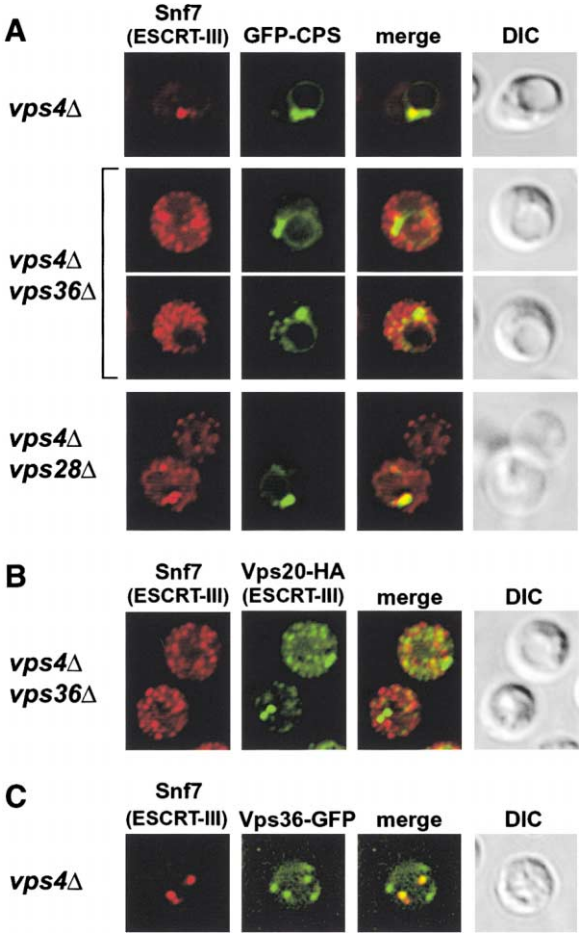

Figure 2. Colocalization of Snf7 with GFP-CPS, Vps20-HA, and Vps36-GFP in Different Yeast Mutants Determined by Immunofluorescence Microscopy

(A) The yeast mutants MBY3 (*vps4*Δ), MBY16 (*vps4*Δ*vps36*Δ), and MBY6 (*vps4*Δ*vps28*Δ) expressing GFP-CPS from the plasmid pGO45 were fixed and stained with antibodies specific for Snf7.

(B) The mutant strain MBY16 (*vps4*Δ*vps36*Δ) expressing Vps20-HA was fixed and stained with antibodies specific for Snf7 and the HA tag.

(C) Colocalization of Snf7 with Vps36-GFP by immunofluorescence microscopy of *vps4*Δ cells carrying chromosomally integrated *VPS36-GFP* (MBY56).

ESCRT-II Associates with Endosomes

Subcellular fractionation revealed that in wild-type cells, the majority of ESCRT-II is found in the soluble pool. However, in cells deleted for *VPS4*, the ESCRT-II protein complex accumulated in the membrane-bound pellet fraction (Figure 1B). This indicated that ESCRT-II transiently associates with membranous compartments and that the dissociation of the protein complex from this compartment is impaired in *vps4*Δ cells. To identify the target compartment of ESCRT-II, a functional *VPS36-GFP* fusion was constructed and integrated into the *VPS36* locus of a number of yeast strains. Consistent with the fractionation data, fluorescence microscopy of these strains revealed that in wild-type cells, Vps36-GFP was localized mainly in the cytoplasm, whereas in *vps4*Δ cells, Vps36-GFP accumulated at large perivacuolar structures, most likely class E compartments (Figure 4A). To support the endosomal localization, *vps4*Δ

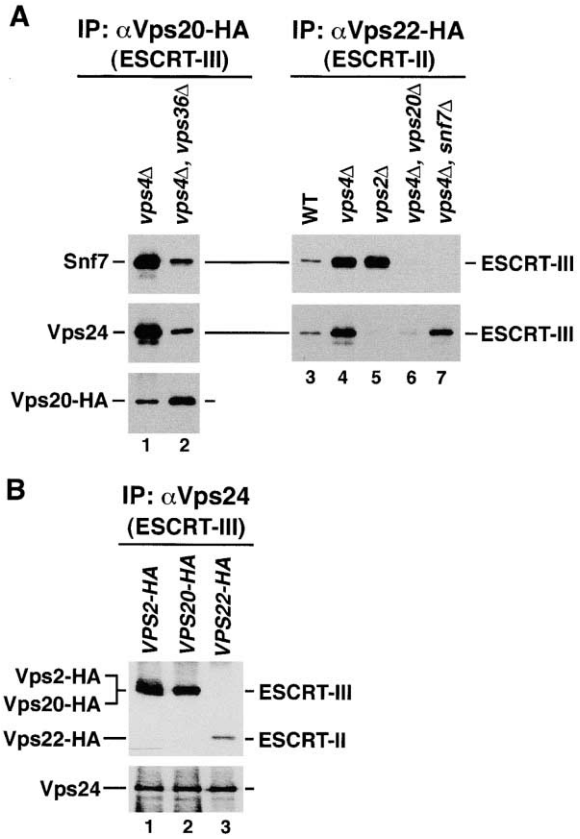

Figure 3. ESCRT-II Physically Interacts with ESCRT-III Subunit Vps20 to Promote ESCRT-III Formation

(A) Detergent-solubilized membranes of wild-type and mutant yeast cells expressing either *VPS20-HA* or *VPS22-HA* were subjected to immunoprecipitation experiments under native conditions using antibodies specific for the HA tag (IP: αVps20-HA; IP: αVps22-HA). The resulting samples were analyzed by Western blot for the presence of ESCRT-III subunits.

(B) Detergent-solubilized membranes of *vps4Δ* cells expressing *VPS2-HA*, *Vps20-HA*, or *Vps22-HA* were used for native immunoprecipitation experiments with antibodies specific for Vps24 (IP: αVps24) and analyzed by Western blot for the presence of the HA-tagged proteins and Vps24.

cells expressing *VPS36-GFP* were subjected to immunofluorescence microcopy using antibodies specific for Snf7, an ESCRT-III subunit which has been shown to associate with endosomes (Babst et al., 1998). The results showed that Vps36-GFP localized to the Snf7-associated compartments (Figure 2C). However, not all structures labeled with Vps36-GFP also stained with anti-Snf7 antibodies, suggesting that membrane association of ESCRT-II does not require the presence of ESCRT-III. Together, the microscopy data indicated that cytoplasmically localized ESCRT-II transiently associates with endosomal compartments and its release from the membrane is dependent on the Vps4 ATPase.

ESCRT-II Physically Interacts with ESCRT-III

The immunofluorescence microscopy demonstrated partial colocalization of ESCRT-III and ESCRT-II, suggesting that these two protein complexes, when associated with endosomal membranes, might physically

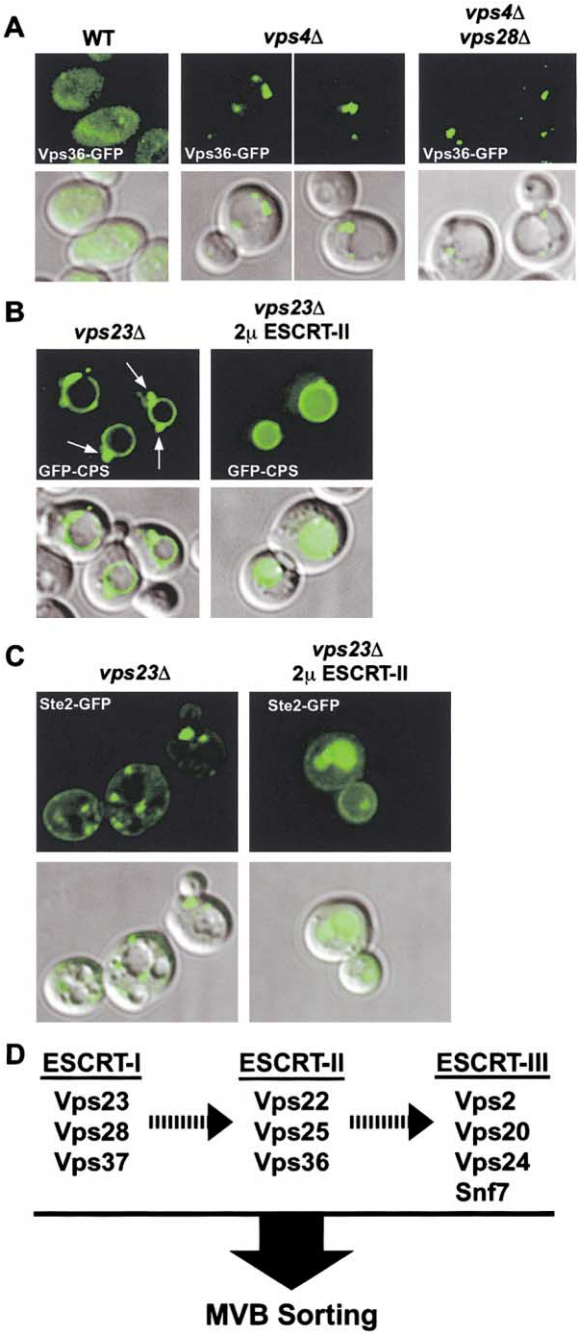

Figure 4. ESCRT-II Accumulates in Class E *vps* Mutants on Endosomal Structures and Functions Downstream of ESCRT-I

(A) Localization of Vps36 by fluorescence microscopy of wild-type and class E *vps* mutant cells containing a chromosomally integrated *VPS36-GFP* fusion (WT: MBY55; *vps4Δ*: MBY56; *vps4Δvps28Δ*: MBY63).

(B) MVB sorting of GFP-CPS, analyzed by fluorescence microscopy, in *vps23Δ* cells, either without (EEY6-2 pGO45) or with the overexpression of ESCRT-II (2μ ESCRT-II: EEY6-2 pGO45, pMB175).

(C) MVB sorting of Ste2-GFP, analyzed by fluorescence microscopy, in *vps23Δ* cells, either without (EEY6-2 pCS24) or with the overexpression of ESCRT-II (2μ ESCRT-II: EEY6-2 pCS24, pMB175).

(D) Order of action of the ESCRT machinery during MVB sorting.

Table 1. Strains and Plasmids Used in this Study

Strain or plasmid	Descriptive name	Genotype or description	Reference or source
S. cerevisiae			
SEY6210	WT	*MATα leu2-3,112 ura3-52 his3-Δ200 trp1-Δ901 lys2-801 suc2-Δ9*	(Robinson et al., 1988)
SEY6210.1	WT	SEY6210, *MAT***a**	(Babst et al., 1997)
MBY28	*vps2Δ*	SEY6210; *vps2Δ1* (*VPS2::HIS3*)	(Babst et al., 2002)
MBY3	*vps4Δ*	SEY6210; *vps4Δ1* (*VPS4::TRP1*)	(Babst et al., 1997)
EEY6-2	*vps23Δ*	SEY6210; *vps23Δ1* (*VPS23::HIS3*)	(Babst et al., 2000)
BWY102	*vps24Δ*	SEY6210; *vps24Δ1* (*VPS24::HIS3*)	(Babst et al., 1998)
MBY30	*vps36Δ*	SEY6210; *vps36Δ1* (*VPS36::HIS3*)	This study
MBY37	*vps4Δvps20Δ*	SEY6210; *vps4Δ1* (*VPS4::TRP1*), *vps20Δ1* (*VPS20::HIS3*)	(Babst et al., 2002)
MBY6	*vps4Δvps28Δ*	SEY6210; *vps4Δ1* (*VPS4::TRP1*), *vps28Δ1* (*VPS28::URA3*)	This study
MBY16	*vps4Δvps36Δ*	SEY6210.1; *vps4Δ1* (*VPS4::TRP1*), *vps36Δ1* (*VPS36::HIS3*)	This study
EEY12	*vps4Δsnf7Δ*	SEY6210; *vps4Δ1* (*VPS4::TRP1*), *snf7Δ1* (*SNF7::HIS3*)	(Babst et al., 2002)
MBY56	*VPS36-GFP*	SEY6210; *VPS36-GFP*, *HIS5* (*S. pombe*)	This study
MBY56	*vps4ΔVPS36-GFP*	SEY6210; *vps4Δ1* (*VPS4::TRP1*), *VPS36-GFP*, *HIS5* (*S. pombe*)	This study
MBY63	*vps4Δvps28Δ VPS36-GFP*	SEY6210; *vps4Δ1* (*VPS4::TRP1*), *vps28Δ1* (*VPS28::URA3*), *VPS36-GFP*, *HIS5* (*S. pombe*)	This study
Plasmids			
pRS425		*LEU2* Ap^R 2μ	(Christianson et al., 1992)
pCS24	Ste2-GFP	*URA3* Ap^R (pRS426) *STE2-GFP*	(Odorizzi et al., 1998)
pGO45	GFP-CPS	*URA3* Ap^R (pRS426) GFP-CPS1	(Odorizzi et al., 1998)
pMB167	*VPS2-HA*	*URA3* Ap^R (pRS416) *VPS2-HA*	(Babst et al., 2002)
pMB168	*VPS20-HA*	*URA3* Ap^R (pRS416) *VPS20-HA*	(Babst et al., 2002)
pMB170	*VPS22-HA*	*URA3* Ap^R (pRS416) *VPS22-HA*	This study
pMB175	2μ ESCRT-II	*LEU2* Ap^R (pRS425) *VPS22-HA*, *VPS25*, *VPS36*	This study
pMB202	ESCRT-II	Ap^R (pET28a+) *VPS22*, *VPS25*, *VPS36*	This study

interact. To test this possibility, the soluble and membrane-bound fractions of yeast strains expressing *VPS22-HA* were subjected to native immunoprecipitation using antibodies specific for the HA tag. The resulting ESCRT-II-enriched fractions were then tested by Western blot for the presence of the ESCRT-III subunits Vps24 and Snf7. The data indicated that the membrane-bound pool of ESCRT-II physically interacts with ESCRT-III (Figure 3A, lane 3). However, no interaction was observed between soluble ESCRT-II and Vps24 or Snf7 (data not shown). As expected, deletion of the dissociating ATPase *VPS4* dramatically increased the amount of ESCRT-III that could be coimmunoprecipitated with Vps22-HA from membranes (Figure 3A, lane 4). This change in ESCRT-II/ESCRT-III ratio suggests that deletion of *VPS4* results in an increased number of ESCRT-III complexes interacting with ESCRT-II and/or in an increased size of ESCRT-III which is associated with ESCRT-II.

ESCRT-III contains two subcomplexes that are formed by the two homologous pairs of class E Vps proteins Vps2-Vps24 and Vps20-Snf7. The Vps20-Snf7 subcomplex is required for membrane association of ESCRT-III, whereas Vps2-Vps24 has been shown to recruit Vps4 which is necessary for disassembly of ESCRT-III (Babst et al., 2002). To test which subcomplex of ESCRT-III interacts with ESCRT-II, several different ESCRT-III mutant strains were subjected to immunoprecipitation experiments. Deletion of *VPS2*, which has been shown to cause accumulation of the Vps20-Snf7 subcomplex on endosomes (Babst et al., 2002), resulted in an increased amount of Snf7 coimmunoprecipitated with ESCRT-II (Figure 3A, lane 5). This result suggested that the interaction between ESCRT-III and ESCRT-II does not require the Vps2-Vps24 subcomplex. In contrast, deletion of *SNF7* in a *vps4Δ* strain resulted in partial loss of ESCRT-II/ESCRT-III interaction, whereas deletion of *VPS20* in *vps4Δ* cells completely abolished the interaction between the two protein complexes (Figure 3A, lanes 6 and 7). Therefore, on the endosomal membrane, ESCRT-II seems to bind to ESCRT-III via Vps20. However, based on the presented data it is not clear whether the Vps20-ESCRT-II interaction is direct or indirect via another unknown protein.

For further characterization of the ESCRT-II/ESCRT-III complex, *vps4Δ* cells expressing HA-tagged ESCRT-III subunits (Vps2-HA and Vps20-HA) or the ESCRT-II subunit (Vps22-HA) were subjected to native immunoprecipitation experiments using antibodies specific for Vps24 (Figure 3B). Anti-HA Western blot analysis demonstrated that the resulting samples contained similar amounts of Vps2-HA and Vps20-HA (ESCRT-III), which is consistent with the finding that ESCRT-III contains approximately the same number of each subunit (Babst et al., 2002). In contrast, Vps22-HA was at least 10-fold less abundant than the ESCRT-III subunits (Figure 3B, compare lane 3 to lanes 1 and 2). However, immunoprecipitation experiments using antibodies specific for ESCRT-II or ESCRT-III have resulted in similar amounts of the ESCRT-III subunits Vps24 and Snf7 (Figure 3A), indicating that the interaction between these two ESCRT complexes is stable. Therefore, the data shown in Figure 3B suggests that for each ESCRT-II within the ESCRT-II/ESCRT-III complex there are numerous ESCRT-III subunits present. This ESCRT-II/ESCRT-III stoichiometry is also reflected in the expression levels of the corresponding subunits. The total cellular levels of ESCRT-II were found to be at least 10-fold lower than those of

the ESCRT-III subunits (data not shown), which explains the weak Vps22-HA bands in the control lanes of the immunoprecipitation experiments (data not shown).

In summary, our data suggest that the interaction between ESCRT-II and Vps20 (ESCRT-III subunit) plays an important role in the formation of ESCRT-III. Interestingly, one of the ESCRT-II subunits, Vps22, is an ~30 kDa protein with two predicted coiled-coil domains and therefore resembles the structure of Snf7. Thus, it is tempting to speculate that Vps20 binds to ESCRT-II via coiled-coil interactions with Vps22 in a fashion similar to the Vps20-Snf7 interaction. Together, the data support a model in which ESCRT-II functions as a nucleation site for the oligomerization of Vps20 and Snf7 on the endosomal membrane and thereby regulates the localization and formation of ESCRT-III. Consistent with this model, whereas proper ESCRT-III localization requires ESCRT-II function, we found that membrane association of ESCRT-II is independent of ESCRT-III (*vps4*Δ*vps20*Δ and *vps4*Δ*snf7*Δ, Figure 1B), further supporting the upstream regulatory role of ESCRT-II. The only class E *vps* mutants found to affect membrane association of Vps22 were strains carrying mutations in other ESCRT-II subunits (*vps4*Δ*vps36*Δ, Figure 1B).

ESCRT-I Functions Upstream of ESCRT-II

ESCRT-I, a protein complex composed of three class E Vps proteins (Vps23, Vps28, and Vps37), functions in the recognition and binding of ubiquitinated endosomal cargo which ultimately results in sorting of the bound cargo proteins into the MVB pathway (Katzmann et al., 2001). Similar to other class E *vps* mutants, loss of ESCRT-I function impairs formation of MVBs. As a consequence, ESCRT-I mutants accumulate endosomal cargo such as GFP-CPS in aberrant endosomal structures, the class E compartments, and mislocalize cargo destined for the vacuolar lumen to the vacuolar limiting membrane. Interestingly, we found that overexpression of all three subunits of ESCRT-II resulted in partial suppression of the ESCRT-I deletion phenotype. In *vps23*Δ cells overexpressing ESCRT-II, GFP-CPS did not accumulate in large perivacuolar structures and was partially transported to the vacuolar lumen (Figure 4B). We also tested whether the delivery of endocytic cargo into MVB vesicles could be suppressed in *vps23*Δ cells by overexpression of ESCRT-II. Downregulation of the α factor receptor Ste2 is known to occur via entry into the MVB pathway (Odorizzi et al., 1998). It can be seen that failure to deliver Ste2-GFP to the lumen of the vacuole in a *vps23*Δ mutant is largely suppressed by overexpression of ESCRT-II (Figure 4C). In contrast, overexpression of ESCRT-I did not suppress the trafficking defect of an ESCRT-II mutant strain (data not shown). Together, these suppression data suggest that ESCRT-I functions upstream of ESCRT-II.

Immunofluorescence microscopy showed that deletion of the ESCRT-I subunit *VPS28* in a *vps4*Δ strain partially impaired accumulation of Snf7 (ESCRT-III) on endosomal structures (marked by GFP-CPS), indicating that ESCRT-III formation was inefficient but not blocked in this mutant background (Figure 2A). In addition, accumulation of ESCRT-II on endosomal structures in *vps4*Δ*vps28*Δ cells was not affected, suggesting that ESCRT-I does not regulate ESCRT-II membrane recruitment (Figure 4A). Furthermore, coimmunoprecipitation experiments did not reveal a physical interaction between ESCRT-II and ESCRT-I. Together, the data suggest a model in which ESCRT-I bound to ubiquitinated cargo activates endosome-associated ESCRT-II in some way and that this regulation is mediated by transient or indirect interactions. In turn, activated ESCRT-II initiates the recruitment and assembly of ESCRT-III through binding to the ESCRT-III subunit Vps20, which ultimately results in the sorting of the cargo molecules into the forming vesicles of the MVB (Figure 4D; see model in Babst et al., 2002).

Experimental Procedures

Materials

Monoclonal antibodies specific for the HA (hemagglutinin) epitope were purchased from Boehringer Mannheim. Polyclonal antiserum against Snf7 and Vps24 has been characterized previously (Babst et al., 1998).

Strains and Media

S. cerevisiae strains used in this work are listed in Table 1. Yeast strains were grown in standard yeast extract-peptone-dextrose (YPD) or synthetic medium supplemented with essential amino acids as required for maintenance of plasmids (YNB; Sherman et al., 1979). The mutant strains MBY23 and MBY30 were constructed by transforming the SEY6210 wild-type strain with a DNA fragment containing the *HIS3* gene flanked by 50 bp specific for the upstream and downstream region of the corresponding gene. The double mutants MBY6 and MBY16 were constructed by transforming the single *HIS3* marked knockouts with a DNA fragment containing the *TRP1* gene flanked by ~200 bp of *VPS4* upstream and downstream DNA (*vps4*Δ*1*). The strains MBY55 and MBY56 were constructed by integrating a *VPS36-GFP* fusion into the chromosome of SEY6210 or MBY3, respectively, using the method described by Longtine et al. (1998). Yeast cells were selected for the presence of the *TRP1* or *HIS3* gene and the deletions and gene fusions were confirmed by PCR analysis of the chromosomal DNA.

DNA Manipulations

Recombinant DNA work was performed using standard protocols (Sambrook et al., 1989). Transformation of *S. cerevisiae* was done by the lithium acetate method as described (Ito et al., 1983). The plasmids used in this study are listed in Table 1. The *VPS22-HA* fusion was constructed by chromosomal integration of the HA tag into the *VPS22* locus using the method described (Longtine et al., 1998). The chromosomal DNA of the resulting strain was used as a template for PCR amplification of the *VPS22-HA*-containing DNA region. This DNA fragment was integrated into the SalI/SpeI-digested pRS416 vector resulting in pMB170. A 1.1 kb NdeI fragment from the library plasmid containing *VPS25* was blunted and cloned into the SmaI-cut pRS425. The resulting plasmid was digested with PstI/XhoI and ligated with a PstI/XhoI-cut PCR fragment containing *VPS36*. This plasmid was cut with NotI, blunted, and cut with SpeI and ligated with a *VPS22-HA*-containing fragment which was obtained by digesting pMB170 with SalI, blunting, and cutting with SpeI. The resulting plasmid containing all three ESCRT-II genes is called pMB175.

Biochemical Assays and Microscopy

For gel filtration analysis, yeast cells were spheroplasted and lysed in PBS (8 g/l NaCl, 0.2 g/l KCl, 1.44 g/l Na_2HPO_4, 0.24 g/l KH_2PO_4 [pH 7.2]) containing 0.1 mM AEBSF (Calbiochem-Novabiochem) and protease inhibitor cocktail (Complete; Roche Molecular Biochemicals). The lysate was centrifuged at 100,000 × g and the resulting supernatant (~2 mg protein) was loaded on a Sephacryl S200 column (16/60; Amersham Life Sciences) and separated in the presence of PBS. Native immunoprecipitation and immunofluorescence experiments were performed as described (Babst et al., 1998, 2002).

Acknowledgments

We wish to thank Eden Estepa-Sabal for technical support. We also wish to thank Drs. Chris Stefan and Tamara Darsow for critical reading of the manuscript and members of the Emr lab for constructive comments. Thanks to Drs. Joan and Ron Conaway for sharing results prior to their publication. This work was supported by a grant from the NIH to S.D.E. (CA58689), a fellowship from the Howard Hughes Medical Institute (M.B.), and a fellowship from the American Cancer Society (D.J.K.). S.D.E. is supported as an Investigator of the Howard Hughes Medical Institute.

Received: January 7, 2002
Revised: June 3, 2002

References

Babst, M., Sato, T.K., Banta, L.M., and Emr, S.D. (1997). Endosomal transport function in yeast requires a novel AAA-type ATPase, Vps4p. EMBO J. *16*, 1820–1831.

Babst, M., Wendland, B., Estepa, E.J., and Emr, S.D. (1998). The Vps4p AAA ATPase regulates membrane association of a Vps protein complex required for normal endosome function. EMBO J. *17*, 2982–2993.

Babst, M., Odorizzi, G., Estepa, E.J., and Emr, S.D. (2000). Mammalian tumor susceptibility gene 101 (TSG101) and the yeast homologue, Vps23p, both function in late endosomal trafficking. Traffic *1*, 248–258.

Babst, M., Katzmann, D.J., Estepa, E.J., Meerloo, T., and Emr, S.D. (2002). ESCRT-III: an endosome-associated heterooligomeric protein complex required for MVB sorting. Dev. Cell *3*, this issue, 271–282.

Christianson, T.W., Sikorski, R.S., Dante, M., Shero, J.H., and Hieter, P. (1992). Multifunctional yeast high-copy-number shuttle vectors. Gene *110*, 119–122.

Felder, S., Miller, K., Moehren, G., Ullrich, A., Schlessinger, J., and Hopkins, C.R. (1990). Kinase activity controls the sorting of the epidermal growth factor receptor within the multivesicular body. Cell *61*, 623–634.

Ito, H., Fukuda, Y., Murata, K., and Kimura, A. (1983). Transformation of intact yeast cells treated with alkali cations. J. Bacteriol. *153*, 163–168.

Kamura, T., Burian, D., Khalili, H., Schmidt, S.L., Sato, S., Liu, W.J., Conrad, M.N., Conaway, R.C., Conaway, J.W., and Shilatifard, A. (2001). Cloning and characterization of ELL-associated proteins EAP45 and EAP20. A role for yeast EAP-like proteins in regulation of gene expression by glucose. J. Biol. Chem. *276*, 16528–16533.

Katzmann, D.J., Babst, M., and Emr, S.D. (2001). Ubiquitin-dependent sorting into the multivesicular body pathway requires the function of a conserved endosomal protein sorting complex, ESCRT-I. Cell *106*, 145–155.

Lemmon, S.K., and Traub, L.M. (2000). Sorting in the endosomal system in yeast and animal cells. Curr. Opin. Cell Biol. *12*, 457–466.

Longtine, M.S., McKenzie, A., III, Demarini, D.J., Shah, N.G., Wach, A., Brachat, A., Philippsen, P., and Pringle, J.R. (1998). Additional modules for versatile and economical PCR-based gene deletion and modification in *Saccharomyces cerevisiae*. Yeast *14*, 953–961.

Luo, W., and Chang, A. (2000). An endosome-to-plasma membrane pathway involved in trafficking of a mutant plasma membrane ATPase in yeast. Mol. Biol. Cell *11*, 579–592.

Odorizzi, G., Babst, M., and Emr, S.D. (1998). Fab1p PtdIns(3)P 5-kinase function essential for protein sorting in the multivesicular body. Cell *95*, 847–858.

Robinson, J.S., Klionsky, D.J., Banta, L.M., and Emr, S.D. (1988). Protein sorting in *Saccharomyces cerevisiae*: isolation of mutants defective in the delivery and processing of multiple vacuolar hydrolases. Mol. Cell. Biol. *8*, 4936–4948.

Sambrook, J., Fritsch, E.F., and Maniatis, T. (1989). Molecular Cloning: A Laboratory Manual, Second Edition (Cold Spring Harbor, NY: Cold Spring Harbor Laboratory Press).

Sherman, F., Fink, G.R., and Lawrence, L.W. (1979). Methods in Yeast Genetics: A Laboratory Manual (Cold Spring Harbor, NY: Cold Spring Harbor Laboratory Press).

Urbanowski, J.L., and Piper, R.C. (2001). Ubiquitin sorts proteins into the intralumenal degradative compartment of the late-endosome/vacuole. Traffic *2*, 622–630.

Yeghiayan, P., Tu, J., Vallier, L.G., and Carlson, M. (1995). Molecular analysis of the *SNF8* gene of *Saccharomyces cerevisiae*. Yeast *11*, 219–224.